

Northumbria Research Link

Citation: Shahkamrani, Arian, Askarian-Abyaneh, Hossein, Nafisi, Hamed and Marzband, Mousa (2021) A framework for day-ahead optimal charging scheduling of electric vehicles providing route mapping: Kowloon case study. *Journal of Cleaner Production*, 307. p. 127297. ISSN 0959-6526

Published by: Elsevier

URL: <https://doi.org/10.1016/j.jclepro.2021.127297>
<<https://doi.org/10.1016/j.jclepro.2021.127297>>

This version was downloaded from Northumbria Research Link:
<http://nrl.northumbria.ac.uk/id/eprint/46109/>

Northumbria University has developed Northumbria Research Link (NRL) to enable users to access the University's research output. Copyright © and moral rights for items on NRL are retained by the individual author(s) and/or other copyright owners. Single copies of full items can be reproduced, displayed or performed, and given to third parties in any format or medium for personal research or study, educational, or not-for-profit purposes without prior permission or charge, provided the authors, title and full bibliographic details are given, as well as a hyperlink and/or URL to the original metadata page. The content must not be changed in any way. Full items must not be sold commercially in any format or medium without formal permission of the copyright holder. The full policy is available online: <http://nrl.northumbria.ac.uk/policies.html>

This document may differ from the final, published version of the research and has been made available online in accordance with publisher policies. To read and/or cite from the published version of the research, please visit the publisher's website (a subscription may be required.)

A Framework for Day-ahead Optimal Charging Scheduling of Electric Vehicles Providing Route Mapping: Kowloon Case Study

Arian Shahkamrani^a, Hossein Askarian-abyaneh^a, Hamed Nafisi^a, M. Marzband^{b,c}

^aDepartment of Electrical Engineering, Amirkabir University of Technology, Tehran, Iran

^bNorthumbria University, Electrical Power and Control Systems Research Group, Ellison Place NE1 8ST, Newcastle upon Tyne, UK

^cCenter of research excellence in renewable energy and power systems, King Abdulaziz University, Jeddah, Saudi Arabia

Abstract

With the ever-increasing growth of electric vehicles (EV)s in the power industry, their significance as a flexible load has increased drastically. On the other hand, uncontrolled charging of these vehicles can cause serious problems in the grid, such as a peak in demand, a decrease in the life expectancy of transformers and as a result, an increase in charging costs of EVs for the EV owners. In this paper, a framework for day-ahead optimal charging of EVs is proposed which through optimization of active and reactive power exchange at each time interval, could prevent the problems mentioned above and at the same time increase the benefit of EV owners and network operators simultaneously. Furthermore, taking into account the effective factors on electrical energy consumption of EVs and the driving pattern of their owners, a route mapping algorithm is developed based on the proposed framework, so as to provide the EV owners with better services. The simulations are carried out using a hybrid interior-point optimization approach, based on traffic and geographic data collected from the city of Kowloon and a standard IEEE 33 bus system is used. The simulation results show that integrating optimal charging of EVs with a route mapping algorithm into the proposed framework can reduce the loss costs of the network during the hours of EVs' presence in the framework and the selling price

Email address: mousa.marzband@northumbria.ac.uk Corresponding author (M. Marzband)

of electricity to EV owners by 24.93% and 33.6%, respectively in comparison with the uncontrolled mode. Also, the average life expectancy of power transformers is increased by 2.97% in the optimal charging mode compared to the uncontrolled mode.

Keywords: Day-ahead scheduling, Electric vehicles, Optimal charging, Route mapping, Transformers loss of life, Cloud storing and computing

Nomenclature

Acronyms

EV	Electric vehicle
PL	Parking lot
EV2G	Electric vehicle to grid
G2EV	Grid to electric vehicle
EV2PL	Electric vehicle to parking lot
PL2EV	Parking lot to electric vehicle
PL2G	parking lot to grid
SO	System operator
PLO	Parking lot operator
CSC	Cloud storing and computing
LOL	Loss of life

Indices

k	Iteration index
n	EV index
t	Time interval
p	PL index
b	Bus index
l	Power line index
N	Set of all EVs
B	Set of all busses

\cap Set of all power lines

Parameters

\bar{k}	Maximum number of iterations
μ^{dep}	Average of EVs' departure times from PLs
σ^{dep}	Standard deviation of EVs' departure times from PLs
bc_n	Battery capacity of EV_n
K	Ratio of the transformer load to its nameplate rating, per unit
R	Ratio of the transformer load loss at the rated load to its no-load loss
m, n	Empirically derived exponents to calculate $\Delta\theta_{b,t}^{\text{TO,U}}$ and $\Delta\theta_{b,t}^{\text{H,U}}$ with changes in the load
τ_H/τ_{TO}	Top-oil/HST time constants (h)
ESL	Estimated shelf life of transformers
CC^{T}	Initial cost (purchase price) of transformers (\$)
i_d	Discount rate
k_b	Wear of battery capacity per charge/discharge
E_n^{bat}	Nominal battery capacity of EV_n (kWh)
CC^{B}	Initial cost (initial purchase price) of the EV battery (\$)
SV	Battery's salvage value at the end of its life cycle (\$)
rel_b	Reliability of bus b
pr_t	Cost of electricity over the time interval t (\$)
R_l	Resistance of line l (Ω)
$\bar{V}_b/\underline{V}_b$	Upper/lower bound for the voltage of bus b (V)
\bar{I}_l	Upper bound for the current of line l (A)
$\bar{\text{SoC}}/\underline{\text{SoC}}$	Upper/lower bound for the SoC (%)
$\bar{\gamma}_C/\underline{\gamma}_d$	Upper/lower bound for the rate of charge/discharge of EV battery (kWh)
v	EV speed (km/h)
g	Road grade ($^\circ$)
θ^A	Ambient temperature ($^\circ\text{C}$)
w	Wind speed (m/s)
$P_{n,t}^v$	Power consumption of EV_n over the time interval t with respect to vehicle speed (KW)

$E_{n,t}^g/E_{n,t}^\theta$	Percentage of change in electrical energy consumption of EV_n over the time interval t with respect to road grade/ambient temperature
$E_{n,t}^w$	Percentage of change in electrical energy consumption of EV_n over the time interval t with respect to wind speed
$t_{n,p}^i$	Time of departure from the origin for EV_n with destination PL_p
$t_{n,p}^{dri}$	Time spent on the road for EV_n with destination PL_p
$t_{n,p}^{ar}/t_{n,p}^{dep}$	Time of arrival/departure of EV_n at/from PL_p
SoC_n^i	Initial SoC of EV_n at the time of departure from the origin (%)
E_n^{dri}	Energy consumption of EV_n along its path (while driving) (kWh)
$SoC_{n,p}^{ar}$	SoC of EV_n at the time of its arrival at PL_p (%)
E_n^{dri}	Electrical energy consumption of EV_n while driving (kWh)
Y_{ba}	Admittance amplitude between buses a and b (\mathcal{U})
θ_{ba}	Angle of voltage between buses a and b ($^\circ$)

Decision Variables

X^k	Location of search agents in iteration k
V^k	Speed of search agents in iteration k
$\Delta\theta_{b,t}^{TO,U}/\Delta\theta_{b,t}^{TO,R}$	Ultimate/rated top-oil temperature rise over ambient temperature for a transformer located on bus b over the time interval t ($^\circ\text{C}$)
$\Delta\theta_{b,t}^H$	HST temperature rise over top-oil temperature for a transformer located on bus b over the time interval t ($^\circ\text{C}$)
$\Delta\theta_{b,t}^{H,U}/\Delta\theta_{b,t}^{H,R}$	Ultimate/rated HST temperature rise over top-oil temperature for a transformer located on bus b over the time interval t ($^\circ\text{C}$)
$\theta_{b,t}^H/\theta_{b,t}^{TO}$	HST/top-oil temperature of transformer located on bus b over the time interval t ($^\circ\text{C}$)

F_{aa}	LOL rate of oil-immersed transformers
F_{EQA}	Equivalent LOL rate of transformers
dbw_n	Average daily battery wear of EV_n (kWh/day)
E_n^-	Electrical energy consumption of EV_n while in V2G mode (kWh)
N_n^{lfc}	Life cycle of the EV_n battery (days)
dwc_n	Daily wear cost of the EV_n battery (\$)
$P_{b,t}/q_{b,t}$	Active/reactive power injected to bus b over the time interval t (kW/kVAR)
$v_{a,t}$	Voltage amplitude of bus a over the time interval t (V)
$\delta_{a,t}$	Phase of bus a over the time interval t ($^\circ$)
$\delta_{b,t}$	Apparent power injected to bus b over the time interval t ($^\circ$)
$I_{l,t}$	Current passing through line l over the time interval t (A)
$p_{n,t}^+/p_{n,t}^-$	Active power exchange from/to the network to/from the EV_n over the time interval t (kW)
$q_{n,t}^+/q_{n,t}^-$	Reactive power exchange from/to the network to/from the EV_n over the time interval t (kVAR)
$en_{n,t}$	Energy required to charge EV_n over the time interval t (kWh)
$SoC_{n,t}$	SoC of EV_n over the time interval t (%)
$U_{n,t}^-/U_{n,t}^+$	Binary variable that indicates if V2G/G2V is activated for EV_n over the time interval t
DLC	Daily energy loss cost of the grid (\$)
DCC	Daily charging costs for EVs (\$)

1. Introduction

2 The increase in greenhouse gas emissions, extensive climate change and most
 3 importantly shortage of fossil fuels has led to the development of alternatives to
 4 fossil-fueled vehicles [1]. The United States environmental protection agency pub-
 5 lished a report in 2018, which shows that transportation services and electricity
 6 generation sectors were two main greenhouse gas sources, releasing almost 55% of
 7 the total emissions in that year [2]. Due to low noise pollution, low greenhouse gas
 8 emissions and also low cost of maintenance, electric vehicles are rapidly expanding

9 as an alternative to fossil-fueled vehicles [3]. Predictions show that the production
10 of EVs will rise by 2040 according to the laws adopted by the governments and
11 people's interest in these vehicles will increase gradually [4]. Therefore, providing
12 better services to EV owners must be more important than ever. Route mapping of
13 EVs considering the lifespan of their batteries and the impact factors on their elec-
14 trical energy consumption is an example of these services [3, 5, 6]. There are a lot
15 of factors that affect the electrical energy consumption of EVs. Vehicle speed, am-
16 bient temperature, wind speed and road grade are among some of these important
17 factors [7]. Electric vehicles are mainly considered as flexible loads in electrical
18 networks. Therefore, they can be controlled in terms of charge/discharge at differ-
19 ent time intervals, preventing peak of demand in the load profile [8]. Controlled
20 charging can also increase the lifespan of power grid transformers and reduce elec-
21 trical energy losses [9]. The benefit of EV owners should also be considered in the
22 controlled charging schedule so that more EVs would want to participate in the
23 schedule [10]. This benefit can be in the form of a reduction in the price of elec-
24 tricity paid for charging EVs, or in the form of an increase in the lifespan of their
25 lithium-ion batteries [11].

26 Furthermore, [12] deals with the charging management of EVs, taking into ac-
27 count wind power and uncertainty in tariff, and utilizes a robust optimization ap-
28 proach in a model predictive framework. In [13] the optimal charging of EVs is
29 performed based on EVs' preferences and concepts from economics. The paper uses
30 the concept of pareto solution to solve a multi-objective optimization problem. [14]
31 examines the benefits of participating in the primary frequency regulation markets
32 for EVs, from the perspective of EV owners. A heuristic-based optimization process
33 is proposed to find an optimized power bid based on local search algorithms. In [15]
34 in addition to the power grid components, the EV transport system is also consid-
35 ered in the problem of charging EVs. A distributed trilayer multi-agent framework
36 is proposed in [16] for optimal EV charging scheduling. The framework reduces the
37 negative effects of EV charging demand on the electrical grids. In [17] parking lots
38 placement is planned long term, considering the simultaneous benefits of the net-
39 work and EV owners. The paper utilizes a multi-objective genetic algorithm to find

40 the optimal location and capacity of EV parking lots, along with the reinforcement
41 plan of the distribution network. In [18] a two-stage approach is developed for
42 EVs' parking lot allocation and DRR (distributed renewable resources), that bene-
43 fits both the network and the parking lot owners. Moreover, genetic algorithm (GA)
44 and particle swarm optimization (PSO) algorithm are used for the distribution net-
45 work loss minimization purpose. Finally, in [19] a method is proposed to determine
46 the optimal siting and sizing of EV parking lots, with the objective of maximizing
47 the profit of electrical distribution companies.

48 Study of previous works in the field of charging and scheduling of EVs exhibit
49 shortcomings (**Sh**) and weaknesses which are divided into the following categories:

- 50 ✓ **Sh1**: day- ahead optimal charging scheduling is based solely on the profit
51 of the EV owners and the benefit of the network operator is not taken into
52 account [1, 3, 13, 14].
- 53 ✓ **Sh2**: day- ahead optimal charging scheduling is based solely on the profit
54 of the network operator and the benefit of the EV owners is not taken into
55 account [4, 6, 9, 15, 16].
- 56 ✓ **Sh3**: In the behavioral modeling of EVs, the SoC and arrival time of EVs at
57 the parking lots are considered without route mapping [6, 12, 17–19].
- 58 ✓ **Sh4**: in the route mapping of EVs, only vehicle speed is considered influen-
59 tial in vehicle's electrical energy consumption and other factors such as road
60 grade, ambient temperature and wind speed are not considered [1, 3, 4].

61 In this paper, a framework for day-ahead optimal charging of EVs is presented
62 based on the optimization of active and reactive power exchange between EVs and
63 parking lots (denoted as EV2PL) and also between parking lots and the network
64 (denoted as PL2G) at each time interval. Furthermore, the benefit of EV owners
65 and system operator are considered simultaneously in this optimization framework.
66 Route mapping is performed for EVs that want to participate in the day-ahead op-
67 timal charging program so as to bring the performance of the proposed framework
68 closer to reality. The route mapping data are then sent to a central control system to
69 communicate with parking lots. Finally, the proposed framework is able to provide
70 services to EVs, PLs and providers in a suitable platform using cloud technology.

71 The main contributions of this paper are summarized as follows:

- 72 ✓ Route mapping for EVs is performed based on four impact factors (vehicle
73 speed, ambient temperature, road grade and wind speed) and as a result, the
74 SoC and arrival time of EVs at the parking lots are determined accordingly
75 (tackling **Sh3** and **Sh4**).
- 76 ✓ Reactive power compensation is considered and subsequently, the loss costs
77 of EVs during charging are reduced (tackling **Sh1**).
- 78 ✓ An optimal charging framework is proposed considering the simultaneous
79 profit of EV owners and system operators (tackling **Sh1** and **Sh2**).
- 80 ✓ The lifespan of EV batteries and power transformers are taken into account
81 in the optimal charging framework (tackling **Sh1** and **Sh2**).

82 **2. System framework**

83 In this paper, a framework for optimal charging of EVs is presented based on
84 cloud storing and computing. Several stakeholders can be involved in this frame-
85 work. The main stakeholders and the possible benefits that the proposed framework
86 can provide for them are discussed below.

- 87 ✓ EV user: EV owners who are interested in participating in this program can
88 reap the benefits of this program, including services to find the optimal route
89 to reach their destination, increasing the battery life of EVs and also reducing
90 their charging costs.
- 91 ✓ System Operator (SO): SO is a centralized unit that must have the required
92 authority to retain information received from EV users and PLOs and meet
93 privacy concerns. SO can be a DSO and participating in this program can
94 help reduce the loss costs of EVs during charging and also extend the lifespan
95 of power transformers.
- 96 ✓ Parking lot operators (PLO): PLOs can benefit from this program with the
97 intent to provide services for EVs. As a matter of fact, by encouraging PLOs
98 to participate in the program, SO allocates part of the profit from reduction
99 of electricity losses to parking lot owners as a privilege. Furthermore, each

100 parking lot can improve the quality of its service by providing information
 101 (such as capacity, selling price, etc.) to EV owners. Moreover, through better
 102 participation in the competitive power market and deployment of different
 103 modes of EVs, PLOs can determine the price of their services such that they
 104 can provide services to more EVs and as a result, their final profit is increased.

105 There are several modes for EVs:

- 106 ✓ Electric vehicle to grid (EV2G)
- 107 ✓ Grid to electric vehicle (G2EV)
- 108 ✓ Vehicle to parking lot (EV2PL)
- 109 ✓ PL to vehicle (PL2EV)

110 These modes cause more EVs to interact with the grid and thus provide more
 111 control over this flexible load. In order to coordinate and enable data exchange
 112 between the involved stakeholders for day-ahead optimal charging, a framework is
 113 proposed, as shown in Figure 1.

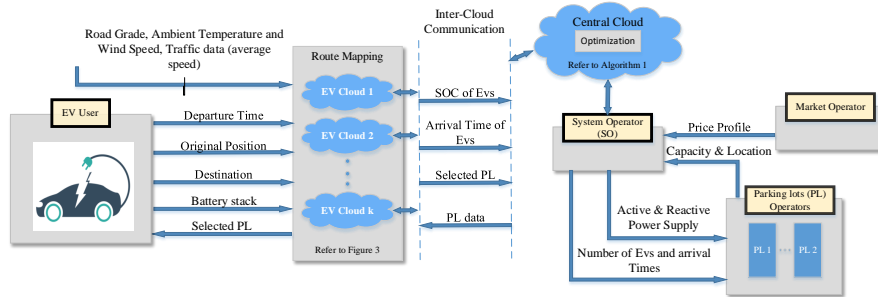


Figure 1: Proposed framework for day-ahead optimal charging of EVs

114 In this framework, the urban network is partitioned into k separate areas and
 115 each area is assigned a cloud to store and process EV data. Moreover, SO receives
 116 relevant and important information from PLOs (such as parking lot location, ca-
 117 pacity, etc.) and from the market operator (the forecasted day-ahead price profile
 118 based on the load profile), and sends this information to a central cloud. First, EV
 119 owners who want to participate in this program send their origin, destination and
 120 time of departure to the EV cloud. This data is sent to one of the area clouds based

121 on the location of EVs throughout the city. Then, according to the destinations spec-
122 ified by the EV owners and the information from the parking lots (capacity, location,
123 etc.), route mapping is performed and the appropriate parking lot for each EV and
124 the proposed route is sent to the EV owners. The appropriate parking lots are se-
125 lected with respect to travel distance. In other words, the nearest parking lot, with
126 available spots, to the destination specified by each EV is determined for that EV via
127 route mapping. In addition, based on the performed route mapping, the estimated
128 SoC of each EV and its estimated arrival time at the selected parking lot(s) are sent
129 to the central cloud. Once this is done for all EVs participating in the day-ahead
130 program, taking into account the benefit of SO and EV owners simultaneously, as
131 well as the constraints related to the charging of EVs, an optimization problem is
132 solved in the central cloud for the next day, using a hybrid interior-point method, so
133 as to determine the optimal active and reactive power exchange between the EVs
134 and the grid at each time interval. Finally, the optimized power and the number
135 of EVs that intend to participate in this program are announced to the PLOs by the
136 SO. EV owners' preferences are also taken into consideration in that the nearest
137 parking lot to their destination is selected for them, which reduces their travel dis-
138 tance and consequently, their travel time and energy consumption are reduced as
139 well. Furthermore, EV drivers determine their arrival/departure times to/from the
140 parking lots and the optimal charging program is developed in such a way that EVs
141 will leave the parking lots with full charge.

142 2.1. *Cloud Storing and Computing (CSC)*

143 This section explains in detail how CSC works. As shown in Figure 2, in gen-
144 eral, cloud storing and computing is a model that allows easy and quick access
145 to a shared pool of configurable computing resources (such as networks, servers,
146 storage, applications and services) with minimal management or service provider
147 interaction [20]. These resources are accessed via the internet, which is metaphori-
148 cally referred to as a "cloud". The focus of this model is to provide on-demand
149 resources for the users, without the need for the user to have special equipment for
150 processing or even be aware of the location of the processing [21].

151 Cloud-based computing allows the user to take advantage of a huge virtual space
152 for storing data and processing them quickly. In addition, it provides a suitable plat-
153 form for quick bidirectional exchange of data between different units [20]. On the
154 other hand utilization of cloud storing and computing, poses some challenges such
155 as information security, ease of access and data management. Cloud data security
156 is usually provided using encryption protocols. This would allow encrypted data to
157 be sent to the cloud. Hence computations in the cloud are performed only on en-
158 crypted data and the results are obtained by decrypting the output sent back from
159 the cloud. However, encryption methods are limited in terms of the types of com-
160 putation they can support; therefore, alternative methods such as transforming the
161 original computational problem, introducing noise into the problem and splitting
162 the original problem and solving each subproblem in a different cloud platform are
163 presented [22]. Confidentiality and integrity of communications to and from the
164 cloud, and within the cloud can also be ensured by standard cryptographic proto-
165 cols such as IPSec or TLS. The issue of access and management of large amounts
166 of data can also be solved by distributing the data and computations between mul-
167 tiple independent clouds. Additionally, the multi-instance architecture minimizes
168 the impact of possible outages and security breaches, since in the case of such oc-
169 currences, not all EVs' data would be compromised. However, this approach results
170 in higher costs for data maintenance and management of each cloud [23]. In this
171 paper, due to the presence of multiple units and the need for communication and
172 processing of large amounts of data, the proposed framework for day-ahead optimal
173 charging of EVs utilizes cloud storing and computing.

174 Each unit in this framework is able to send or receive real-time information to
175 or from the cloud server using an application. To this end, each EV user is able to
176 log in to the application through a pre-assigned user id and password, and share
177 its required information such as type of battery and its capacity, SoC of the battery,
178 vehicle speed, etc. with the cloud. The cloud then uses this information, along with
179 the information it receives from the operators of other units (PLOs), to provide the
180 EV users with the closest parking lot and the suggested route to the selected parking
181 lot, through the application.

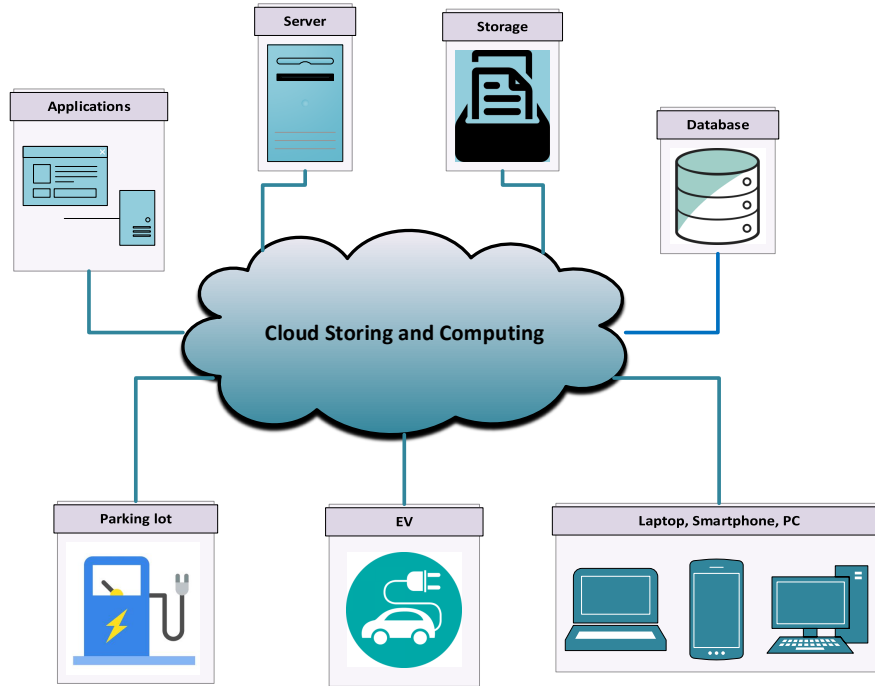


Figure 2: Cloud storing and computing

182 *2.2. Route Mapping*

183 In this section, the route mapping performed in the EV cloud is discussed. Route
 184 mapping of EVs, as one of the main future means of transportation, is a very im-
 185 portant issue and faces many challenges (such as limited capacity of EV batteries,
 186 sparse availability of charging stations and time-consuming process of charging EVs)
 187 [24]. Therefore, several route mapping approaches consider optimizing energy con-
 188 sumption explicitly. However, energy optimal routes often greatly increase travel
 189 time and so optimizing energy consumption as single criterion is helpful only in
 190 special cases, e.g., when the battery SoC is very low. In practice, users would be
 191 more interested in taking routes that form a convenient trade-off between travel
 192 time and energy consumption.

193 It should also be noted that in reality, in most urban environments, EVs consti-
 194 tute the minority of vehicles and most of the urban traffic is made up of conventional

195 cars. Therefore, the route mapping in this paper is performed taking into account
196 the presence of these conventional vehicles. Furthermore, the proposed framework
197 for optimal charging of EVs can also be extended to conventional vehicles, where
198 the drivers of these vehicles can participate in a similar program where they can be
199 informed of the nearest gas station to their destination, gas station capacity, fuel
200 costs, etc.

201 Dijkstra's algorithm is one of the most widely used routing algorithms, which
202 is utilized in this paper. In 1959, Dijkstra developed an algorithm for the shortest
203 path problem that appeared to be considerably more efficient and required less data
204 storage space compared to the previous methods. This algorithm is a mature classi-
205 cal shortest path of single source algorithm and it is used for calculating the shortest
206 path from one node to all other nodes in non-negative weights graphs [25]. In 1968
207 [26] developed a search strategy called A^* to find the path with the minimum cost.
208 This algorithm is different from other methods since it utilizes an estimate of the cost
209 of "path-completion" and it finds the optimal path for certain classes of estimating
210 functions. In [27], a comparative study was done regarding the performance of Di-
211 jkstra and A^* . The results indicated that A^* can outperform Dijkstra's algorithm
212 with respect to run time when spatial coordinated are present. However, as men-
213 tioned earlier, A^* requires a function for estimating the completion cost of a path
214 and therefore is not suitable for many shortest path applications. Another famous
215 method of the shortest path algorithm is the Floyd algorithm. [25] investigates the
216 online real-time path planning abilities of Floyd, Dijkstra and A^* under two con-
217 ditions: the threat of fixed obstacles and sudden threats. Although all three can
218 handle fixed and sudden threats, Dijkstra's algorithm is better in terms of the run
219 time, complexity and path length of the three algorithms [25]. Even though Dijkas-
220 tra is one of the earliest developed shortest path algorithms, it remains to this day
221 one of the best approaches for optimally solving the simple shortest path problem
222 when all arcs have non-negative lengths and a lot of research is being conducted to
223 improve and extend Dijkstra [28–30]. Therefore, this algorithm has been applied
224 in many domains and applications, the most famous of which is Google Maps.

225 In this paper, using Dijkstra's algorithm, the shortest path is obtained with re-

226 spect to travel time and then the electrical energy required for traveling the chosen
227 path is calculated according to four impact factors. Vehicle speed is one of the
228 most important impact factors that influence the energy consumption of EVs. In
229 addition, some environmental factors such as wind speed, road grade and ambient
230 temperature can significantly affect EV's energy consumption [7]. This paper takes
231 into account the aforementioned impact factors in determining the required electri-
232 cal energy consumption for each path so as to calculate energy consumption more
233 accurately and improve vehicle fuel economy.

234 *2.2.1. The proposed algorithm for Route Mapping of EVs*

235 This section provides an algorithm based on Dijkstra's method for the route
236 mapping of EVs. The flowchart of the proposed algorithm is shown in Figure 3.

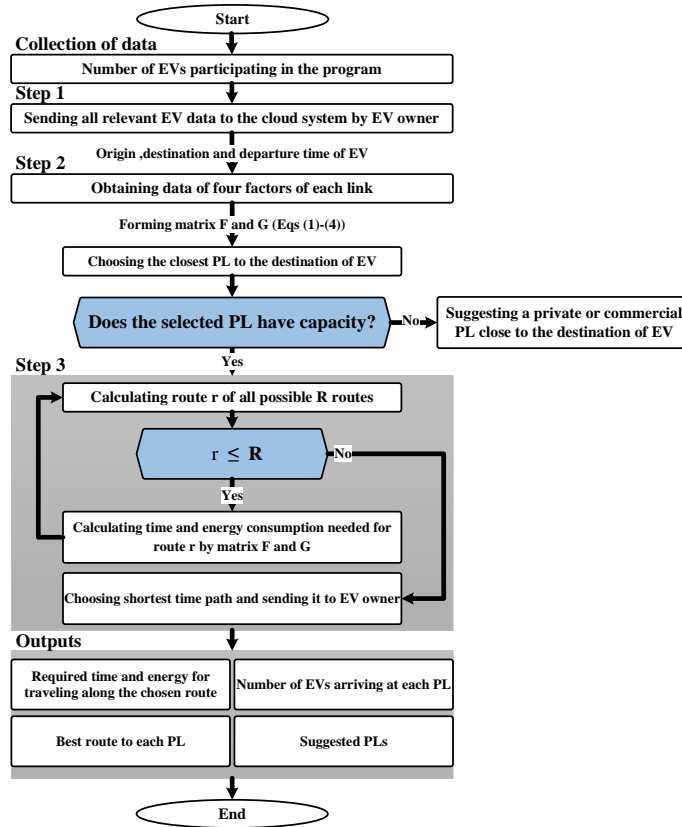


Figure 3: Flowchart of the proposed algorithm for route mapping performed in the EV cloud based on Dijkstra's algorithm

237 An urban network is constituted of a number of links and intersections. First,
 238 the urban network is modeled as a graph in which each link represents a street
 239 and each node represents the intersection of the city's main streets. **Step 1- Step**
 240 **3** are implemented to utilize the proposed algorithm. These steps are described as
 241 follows:

- 242 ✓ **Step 1:** the information about a driver (including the departure time, origin
 243 and destination) that wants to participate in the day-ahead optimal charging
 244 program is sent to the EV cloud so that the appropriate parking lot and the
 245 suggested route to that parking lot are provided for the driver.
- 246 ✓ **Step 2:** given the average speed of EVs in each link and also the length of each

247 link, the estimated time required for traveling each link is obtained and as a
 248 result, matrix $F_n = [f_{n,ij}]_{s \times s}$, which is the travel time matrix of each link is
 249 formed; Where s is the number of nodes in the graph and $f_{n,ij}$ is the required
 250 time for EV_n to reach node j from node i . similarly, the electrical energy
 251 consumption required for each EV to pass through each link is calculated
 252 based on available data and Eqs (5)- (8). Finally, matrix $G_n = [g_{n,ij}]_{s \times s}$
 253 which is the electrical energy consumption matrix passing through each link
 254 is formed. Where s is the number of nodes in the graph and $g_{n,ij}$ is the
 255 required energy for EV_n to reach node j from node i . for example, given $s=$
 256 2 and $n= 2$, matrices F and G are formed as follows:

$$F_1 = \begin{pmatrix} 0 & f_{1,12} \\ f_{1,21} & 0 \end{pmatrix} \quad (1)$$

$$F_2 = \begin{pmatrix} 0 & f_{2,12} \\ f_{2,21} & 0 \end{pmatrix} \quad (2)$$

$$G_1 = \begin{pmatrix} 0 & g_{1,12} \\ g_{1,21} & 0 \end{pmatrix} \quad (3)$$

$$G_2 = \begin{pmatrix} 0 & g_{2,12} \\ g_{2,21} & 0 \end{pmatrix} \quad (4)$$

261 where $f_{1,12}$, $f_{2,12}$, $f_{1,21}$ and $f_{2,21}$ are the required time for EV_1 and EV_2 to reach
 262 node 2 from node 1 and vice versa respectively. Similarly $g_{1,12}$ and $g_{2,12}$ are
 263 the required electrical energy for EV_1 and EV_2 to reach node 2 from node 1
 264 respectively. And $g_{1,21}$ and $g_{2,21}$ are the required electrical energy for EV_1 and
 265 EV_2 to reach node 1 from node 2 respectively. It's evident that the diagonal
 266 entries of F_n and G_n are zero.

267 ✓ **Step 3:** at this stage, all possible routes to reach the destination specified by
 268 the EV owner, are obtained. Assuming that there are R possible routes, the
 269 shortest time path is identified and the travel time and energy consumption
 270 of EVs along the chosen route are calculated based on Eqs (5)-(8). Also, the
 271 suggested parking lot and the best route to each parking lot are presented to

272 each EV accordingly. Furthermore, the number of EVs and their arrival times
 273 to each parking lot are announced to the PLOs. It is worth noting that since
 274 the capacities of the PLs are limited, in a case where the selected parking lot
 275 for some EVs is full, the algorithm suggests another private or commercial
 276 parking lot which is close to the destination of those EVs. Nevertheless, those
 277 EVs are not included in the proposed charging program of this paper. This is
 278 because due to the partitioning of the urban network, the parking lots are lo-
 279 cated relatively far apart, and suggesting another parking lot in the program,
 280 could move some EVs away from their destination.
 281 For instance, Figure 4 demonstrates an urban network containing 6 nodes
 282 $\{a_i\}_{i=1}^6$ and 8 links $\{e_i\}_{i=1}^8$. As shown in the figure, the EV driver is
 283 supposed to travel from a_1 to a_6 . There is a total of 8 different routes between
 284 the two nodes and according to the algorithm demonstrated in Figure 3, the
 285 shortest time route (the red route) and the time and energy required to travel
 286 along this route are obtained.

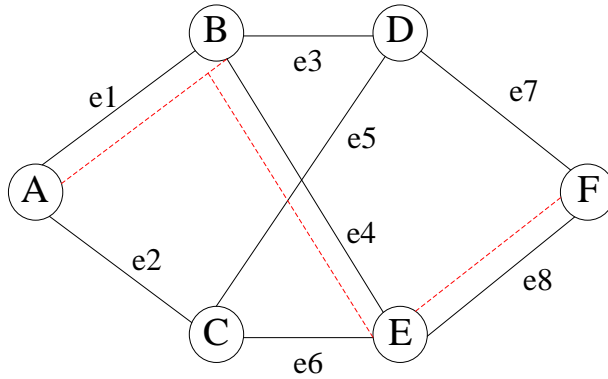


Figure 4: Path graph for EVs to travel from a_1 to a_6

287 **3. Problem Formulation**

288 *3.1. Factors influencing the electrical energy consumption of EVs*

289 Several factors affect the electrical energy consumption of EV batteries. The
290 most important of these factors are vehicle speed, ambient temperature, road grade
291 and wind speed [7, 31]. In the following, each factor is examined separately.

292 *3.1.1. Vehicle speed*

293 The first and most important factor that influences the energy consumption of
294 EVs is vehicle speed. As illustrated in Figure 5, there is a direct relationship between
295 the two parameters of energy consumption and speed of EVs. This relationship is
296 modeled by a third order polynomial function according to Eq (5) [7].

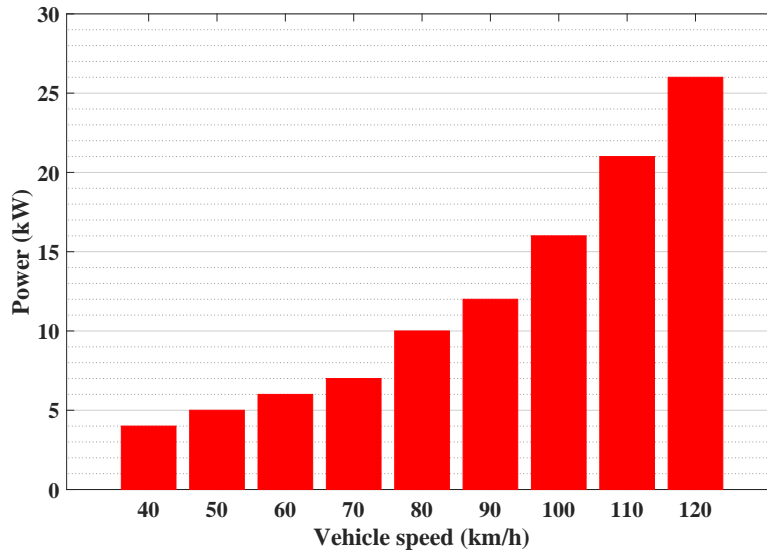


Figure 5: Relationship between energy consumption and speed of EVs

297

$$P_{n,t}^v = 2.247 \times 10^{-5} v_{n,t}^3 - 0.002205 v_{n,t}^2 + 0.1547 v_{n,t} + 0.04653 \quad \forall t \in T, \forall n \in N \quad (5)$$

298 *3.1.2. Road grade*

299 Road grade is another important factor that has a significant effect on the en-
300 ergy consumption of EVs. The relationship between road grade and the energy
301 consumed by EVs is illustrated in Figure 6. Moreover, this relationship is modeled
302 by a third order function according to Eq (6) [7].

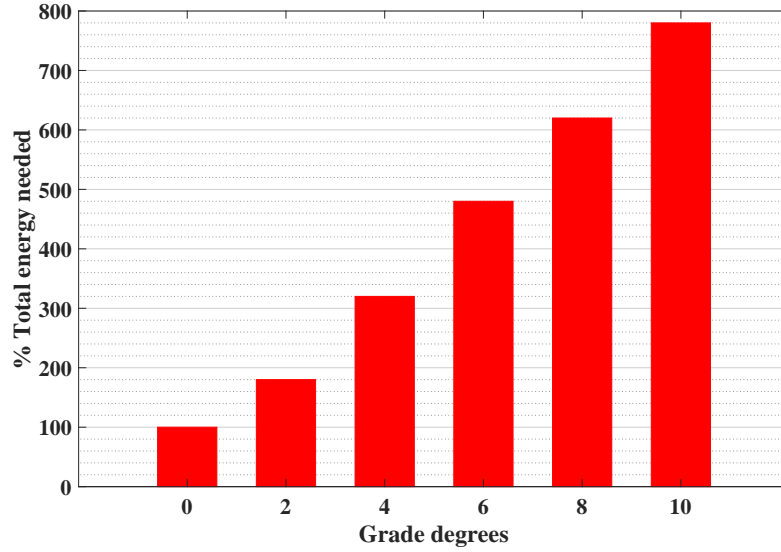


Figure 6: Relationship between percentage of changes in electrical energy consumption of EVs and road grade

303

$$E_{n,t}^g = -0.3067g_{n,t}^3 + 6.721g_{n,t}^2 + 31.77g_{n,t} + 97.54 \quad \forall t \in T, \forall n \in N \quad (6)$$

304 *3.1.3. Ambient temperature*

305 The next factor that influences the energy consumption of EVs is ambient tem-
306 perature. This factor indirectly impacts the electrical energy consumption of EVs
307 by affecting the use of their cooling and heating systems. At ideal temperatures
308 (20°C), the EV owners do not usually see the need to use cooling and heating sys-
309 tems, but with changes in temperature, the need to use these systems is gradually
310 felt. The relationship between ambient temperature and energy consumption of
311 EVs is shown in Figure 7 and modeled by a third order function according to Eq (7)

312 [31].

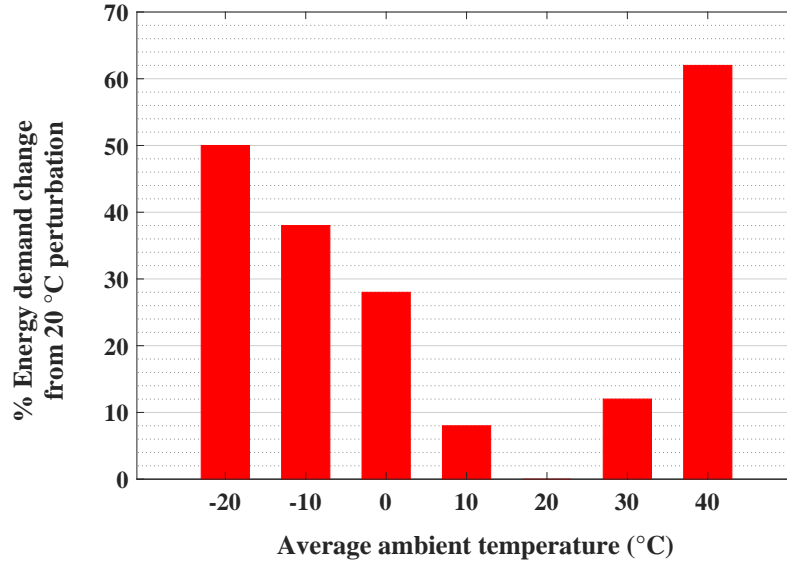


Figure 7: Relationship between percentage of changes in electrical energy consumption of EVs and ambient temperature

313

$$E_{n,t}^{\theta} = 1.875 \times 10^{-3} \theta_{n,t}^3 - 3.532 \times 10^{-3} \theta_{n,t}^2 - 1.951 \theta_{n,t} + 25.33 \quad \forall t \in T, \forall n \in N \quad (7)$$

314 3.1.4. Wind speed

315 Wind speed and direction is another factor that influences the energy consump-
316 tion of EVs. By moving in the direction of the wind, the consumption of electrical
317 energy is decreased whereas moving in the opposite direction has the opposite ef-
318 fect. The relationship between wind speed and energy consumption of EVs is il-
319 lustrated in Figure 8, and modeled by a third order function according to Eq (8)
320 [7].

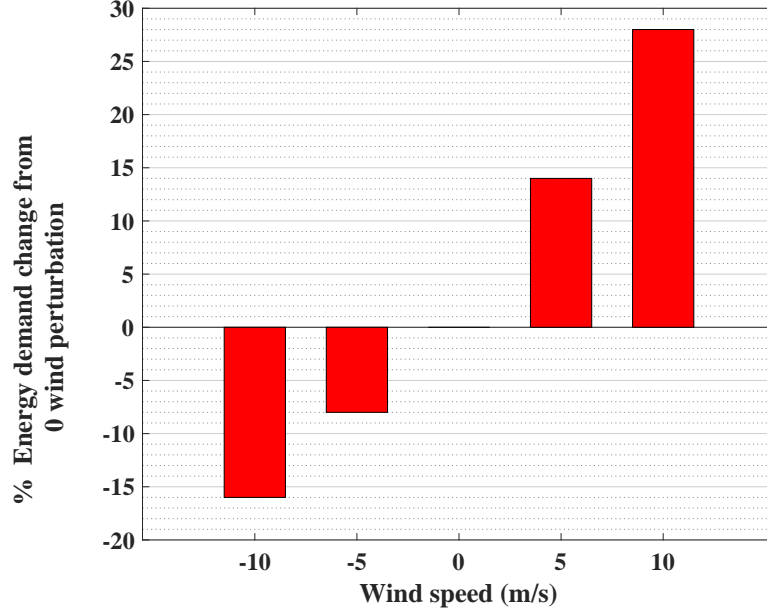


Figure 8: Relationship between percentage of changes in electrical energy consumption of EVs and wind speed

321

$$E_{n,t}^w = 6.77 \times 10^{-18} w_{n,t}^3 + 0.06857 w_{n,t}^2 + 2.2 w_{n,t} + 0.171 \quad \forall t \in T, \forall n \in N \quad (8)$$

322 3.2. Modeling the presence of EVs in parking lots

323 To model the presence of EVs in the parking lots (PLs), in order to schedule
 324 for the optimal exchange of active and reactive power, Eqs (9), (10) and (11) are
 325 used for the calculation of arrival and exit times and SoC of EVs when entering the
 326 PLs, respectively. It should be noted that the departure time of EVs, both from their
 327 origin and from the PLs, are known and sent to the cloud by EV owners beforehand.
 328 In the simulations, however, these values were modeled using the Gaussian model.
 329 The arrival time of EVs to the parking lots, on the other hand, is obtained via route
 330 mapping as was mentioned in step 3 of the route mapping algorithm of section
 331 2.2.1. Furthermore, it is assumed that the EVs are charged from night till morning
 332 and move towards the PLs at full charge (i.e., with an SoC of 80%).

$$t_{n,p}^{ar} = T_{n,p}^{dri} + t_{n,p}^i \quad (9)$$

$$t_{n,p}^{\text{dep}} = \mu^{\text{dep}} + \sigma^{\text{dep}} N_1 \quad (10)$$

$$\text{SoC}_{n,p}^{\text{ar}} = \text{SoC}_n^i - E_n^{\text{dri}}/bc_n \quad (11)$$

3.3. Modeling the thermal behavior of transformers

Thermal transformers are one of the main components of power networks and this section is dedicated to obtaining a thermal model for them [32]. At each time interval the ultimate top-oil temperature rise, as well as the ultimate HST (hottest spot temperature) rise for the transformers of bus 'b' are calculated from the load level at that instant according to Eqs (12) and (13). Then from the ultimate top-oil temperature rise and the ambient temperature at each time interval, the increment in the top-oil temperature is calculated using Eq (14). The increment in the HST rise can also be calculated according to Eq (15).

$$\Delta\theta_{b,t}^{\text{TO,U}} = \Delta\theta_{b,t}^{\text{TO,R}} \times \left(\frac{K^2R + 1}{R + 1} \right)^n \quad \forall b \in B, \quad \forall t \in T \quad (12)$$

$$\Delta\theta_{b,t}^{\text{H,U}} = \Delta\theta_{b,t}^{\text{H,R}} \times K^{2m} \quad \forall b \in B, \quad \forall t \in T \quad (13)$$

$$\tau^{\text{TO}} \frac{d\theta_{b,t}^{\text{TO}}}{dt} = \left(\Delta\theta_{b,t}^{\text{TO,U}} + \theta_t^{\text{A}} \right) - \theta_{b,t}^{\text{TO}} \quad \forall b \in B, \quad \forall t \in T \quad (14)$$

$$\tau^{\text{H}} \frac{d\Delta\theta_{b,t}^{\text{H}}}{dt} = \left(\Delta\theta_{b,t}^{\text{H,U}} - \Delta\theta_{b,t}^{\text{H}} \right) \quad \forall b \in B, \quad \forall t \in T \quad (15)$$

Finally, in order to obtain the HST, the top-oil temperature and the HST rise are added according to Eq (16).

$$\theta_{b,t}^{\text{H}} = \theta_{b,t}^{\text{TO}} + \Delta\theta_{b,t}^{\text{H}} \quad \forall b \in B, \quad \forall t \in T \quad (16)$$

According to ANSI/IEEE standard, the LOL rate of oil-immersed transformers can be calculated using Eq (17).

$$F_{\text{aa}} = \exp \left(\frac{15000}{383} - \frac{15000}{\theta_{\text{H}} + 273} \right) \quad (17)$$

According to this standard Eq (18) is used to obtain the equivalent LOL rate.

$$F_{\text{EQA}} = \frac{\sum_{t=1}^T F_{\text{aa}_t} \Delta t_t}{\sum_{t=1}^T \Delta t_t} \quad (18)$$

As a result, the transformers loss of life (LOL) is calculated using Eq (19).

$$\text{LOL}_T = \frac{\text{ESL}}{F_{\text{EQA}}} \quad (19)$$

359 Now, with the help of engineering economics formulas, the daily operational
 360 cost of transformers is modeled according to Eq (20).

$$\text{DOC} = \frac{\left((1 + i_d)^{\frac{1}{365}} - 1 \right) (1 + i_d)^{\text{LOL}_T}}{\left((1 + i_d)^{\text{LOL}_T} - 1 \right) (1 + i_d)^{1/365}} \times \text{CC}_T \quad (20)$$

362 3.4. Modeling of EVs' batteries

363 Another component that has been modeled in this work is the lifespan of EV
 364 batteries based on their energy exchange with the grid network. This modeling
 365 is based on the equations in [33]. It should be noted that according to [34], the
 366 effect of the current rate at charge rates below 1C, is less than that of the SoC
 367 and can be neglected. Since in the simulations performed, the maximum charge
 368 rate is considered to be 5kWh, which is equivalent to 0.5C, the current rate is not
 369 considered in the modeling of battery lifespan. It is also assumed that all EVs move
 370 from their origin to the parking lots at full battery charge, and eventually their
 371 battery charge reaches its full value when leaving the parking lots, in which case
 372 the average daily wear of EV batteries is modeled using Eq (21).

$$\text{dbw}_n = k_b \left((1 + e) E_n^{\text{dri}} + 2E_n^- \right) \text{ (kW.h) / day} \quad (21)$$

374 where k_b is the wear of battery capacity per charge/discharge in (KWs); which is
 375 equal to 0.0015 (kWh/kWh) according to [33]. i.e. for each charge or discharge of
 376 1 kWh, the capacity of lithium-ion batteries is reduced by 0.00015 kWh. Moreover,
 377 due to the fact that the energy exchanged in V2G mode must eventually be replen-
 378 ished by recharging, E_n^- is multiplied by 2. The weighing factor e is considered due
 379 to the higher energy discharge during driving compared to the V2G mode, which
 380 according to [35] equals 2.22.

381 According to [33], EV batteries reach the end of their lifespan as they lose 20%
 382 of their original nominal capacity and hence the approximate battery life for each
 383 EV is modeled using Eq (22).

$$N_n^{\text{lfc}} = \frac{0.2E_n^{\text{bat}}}{\text{dbw}_n} \text{ (days)} \quad (22)$$

385 Now based on engineering economics formulas, the daily cost due to EV battery
 386 wear is calculated using Eq (23). In this equation, the difference between the initial

387 cost of batteries and their salvage value are spread over the batteries' life cycle, with
 388 the incorporation of i_d . i_d acts as the inflation rate and has to be accounted for to
 389 compare the initial cost and salvage value, in a realistic way.

$$dwc_n = \frac{i_d (CC^B (1 + i_d)^{N_n^{lfc}} - SV)}{(1 + i_d)^{N_n^{lfc}} - 1} \frac{\text{US\$}}{\text{day}} \quad (23)$$

391 3.5. Cost function

392 The cost function consists of two parts. The first part (OF_1) concerns the profit of
 393 EV owners in the day-ahead optimal charging program which includes minimizing
 394 the cost of charging EVs and increasing the lifespan of their batteries whereas the
 395 second part of the cost function (OF_2) concerns the profit of network operators.
 396 These profits include reducing losses and improving the lifespan of the network's
 397 power transformers.

$$\min OF = OF_1 + OF_2 \quad (24)$$

$$OF_1 = \sum_{b \in B} \sum_{t \in T} \sum_{n \in N} rel_b \cdot (en_{n,t} \cdot pr_t) + \sum_{n \in N} dwc_n \quad (25)$$

$$OF_2 = \sum_{t \in T} \sum_{l \in \Omega} R_l I_{l,t}^2 \cdot pr_t + \sum_{b \in B} DOC_b \quad (26)$$

$$P_{b,t} = \sum_{a \in B} V_{b,t} \cdot V_{a,t} \cdot Y_{ba} \cdot \cos(\theta_{ba} - \delta_{b,t} + \delta_{a,t}), \quad \forall b \in B; \forall t \in T \quad (27)$$

$$q_{b,t} = \sum_{a \in B} V_{b,t} \cdot V_{a,t} \cdot Y_{ba} \cdot \sin(\theta_{ba} - \delta_{b,t} + \delta_{a,t}), \quad \forall b \in B; \forall t \in T \quad (28)$$

$$P_{b,t} + jq_{b,t} = S_{b,t}, \quad \forall b \in B; \forall t \in T \quad (29)$$

$$\underline{V}_b \leq V_{b,t} \leq \overline{V}_b, \quad \forall b \in B; \forall t \in T \quad (30)$$

$$I_{l,t} \leq \overline{I}_l, \quad \forall l \in \Omega; \forall t \in T \quad (31)$$

$$\underline{SoC} \leq SOC_{n,t} \leq \overline{SoC}, \quad \forall t \in T, \forall n \in N \quad (32)$$

$$p_{n,t}^+ \leq \overline{\gamma}_c, \quad p_{n,t}^- \leq \overline{\gamma}_d \quad \forall t \in T \quad (33)$$

$$q_{n,t}^+ \leq \overline{\gamma}_c, \quad q_{n,t}^- \leq \overline{\gamma}_d \quad \forall t \in T, \forall n \in N \quad (34)$$

$$U_{n,t}^+ + U_{n,t}^- \leq 1, \quad U_{n,t}^+ + U_{n,t}^- \leq 1 \quad \forall t \in T, \forall n \in N \quad (35)$$

410 Eqs (27)- (31) represent the load distribution constraints and Eqs (32)- (35) on
 411 the other hand, represent the charge/discharge constraints of EVs.

412 3.6. Optimization algorithm

413 In this section, steps of the proposed algorithm for obtaining the optimal active
414 and reactive power exchange between the EVs and the grid, in the day-ahead opti-
415 mal charging program, are illustrated in detail using Algorithm 1. In this algorithm,
416 a hybrid interior-point approach is adopted. The interior-point method, which is a
417 gradient-based optimization algorithm, was used due to the superior performance
418 compared to heuristic optimization approaches [36]. Interior-point methods are
419 very efficient search approaches. However, they require a good starting point in or-
420 der to end up in the global optimum instead of a local optimum [37]. Thus, whale
421 optimization (WO) algorithm was combined with the interior-point method to pro-
422 vide an initial point and help speed up the search. In this hybrid approach, first
423 the WO algorithm, which is a heuristic, is launched and the problem is solved until
424 a termination criterion is met [38]. One possible stopping criterion is a specified
425 maximum number of iterations [39]. The solution is then passed on to the interior-
426 point method as the initial point. Due to the sensitivity of interior-point methods
427 to the starting point, this hybrid approach increases the chance of finding the prob-
428 lem's most likely global solution. The aim of Algorithm 1 is managing the values
429 of p_t^* and q_t^* , which represent the optimal active and reactive power respectively,
430 such that (24) is minimized. Based on the proposed framework of section 2 and
431 the charging constraints of (27)-(35), EVs are charged using this algorithm.

Algorithm 1: The proposed algorithm

- 1 **Input** Route mapping data, EVs characteristics, the forecasted ambient temperature, and electricity price.
- 2 **Output:** Optimal active and reactive power exchange (p_t^* , q_t^*), between EVs and the grid at each interval

Providing the solution obtained by the WO method as the initial point

```

3 while  $|OF_{k+1} - OF_k| > \epsilon$  do
    for each test point  $i \in N_{Pop}$  do
        Updating  $p_t$  and  $q_t$ 
        for each time step  $t \in \tau$  do
            Performing power flow subject to constraints using Eqs (27)- (33)
            Obtaining  $F_{aa}^t$  using Eq (17)
                
$$F_{aa}^{daily} \leftarrow F_{aa}^{daily} + \frac{F_{aa}^t \cdot \Delta t_n}{\sum_{n=1}^T \Delta t_n} \quad (36)$$

            for each power line  $l \in \Omega$  do
                
$$DLC \leftarrow DLC + pr_t \cdot R_l I_{l,t}^2 \quad (37)$$

            end
            for each EV  $n \in N$  do
                
$$SoC_{n,t} \leftarrow SoC_{n,t} + \frac{p_t}{bc_n} \quad (38)$$

            for each bus  $b \in B$  do
                
$$DCC \leftarrow DCC + rel_b \cdot (en_{n,t} \cdot pr_t) \quad (39)$$

            end
            end
            Calculating  $dwc_t$  using Eq (23)
                
$$OF_i \leftarrow DCC + DLC + DCC + dwc_t \quad (40)$$

            if  $OF_{k+1} > OF_i$  then
                
$$OF_{k+1} \leftarrow DOC + DLC + DCC + dwc_t \quad (41)$$

            end
        end
    end
    Forming a new point
end

```

432 4. Case study

433 4.1. Input data

434 In this section, the proposed framework for the day-ahead optimal charging
435 of EVs is implemented with the utilization of Kowloon traffic and weather data

436 [40, 41]. As mentioned in Section 2.2.1, for the route mapping of EVs, a number
437 of nodes are assigned to the intersections of Kowloon's main streets as shown in
438 Figure 9. Furthermore, it is assumed that a total of 7 parking lots are located in
439 different parts of the city and 800 EVs are willing to participate in the day-ahead
440 optimal charging program.

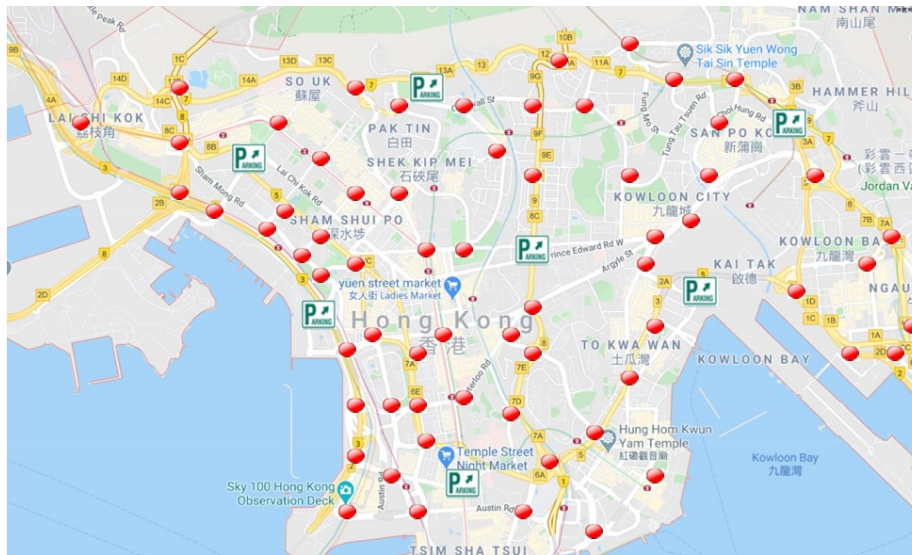


Figure 9: Kowloon city map

441 In order to model the Kowloon power grid, the standard IEEE 33 bus system
442 is used. The electric power grid diagram and the location of the parking lots on
443 the buses are shown in Figure 10. Located on each of these buses is a thermal
444 transformer, whose lifespan is affected by factors such as overload and ambient
445 temperature. Data on thermal transformers and their prices are given in [42].

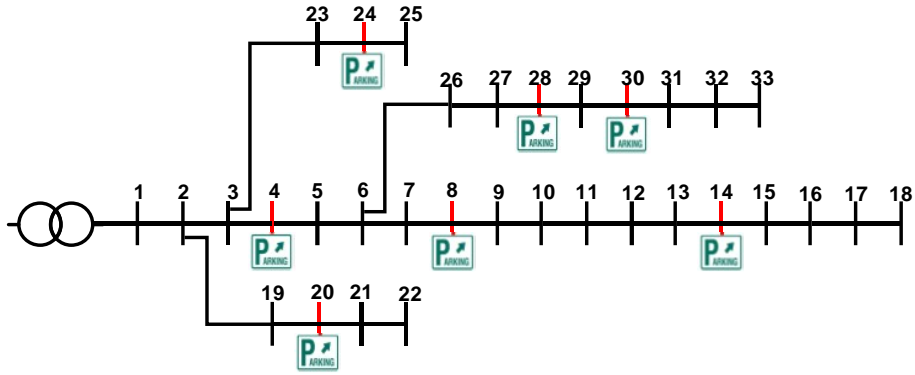


Figure 10: IEEE 33 bus system and the location of PLs

446 The market share percentage of EVs, based on their class specifications is dis-
 447 played in Table 1. Furthermore, according to [43], the price of lithium ion batteries
 448 is estimated at 175 \$/kWh.

Table 1: Market share percentage of EVs based on their class specifications

EV Class	β (kWh)	Market Share
1	10	0.2
2	12	0.3
3	16	0.3
4	21	0.2

449 The data related to the modified electricity price profile based on time of use
 450 (TOU), for warm and cold seasons are collected from [44] and [45] respectively,
 451 and the load profile, for cold and warm seasons are derived from [46]. Moreover,
 452 the electricity price profile is shown in Figure 11.

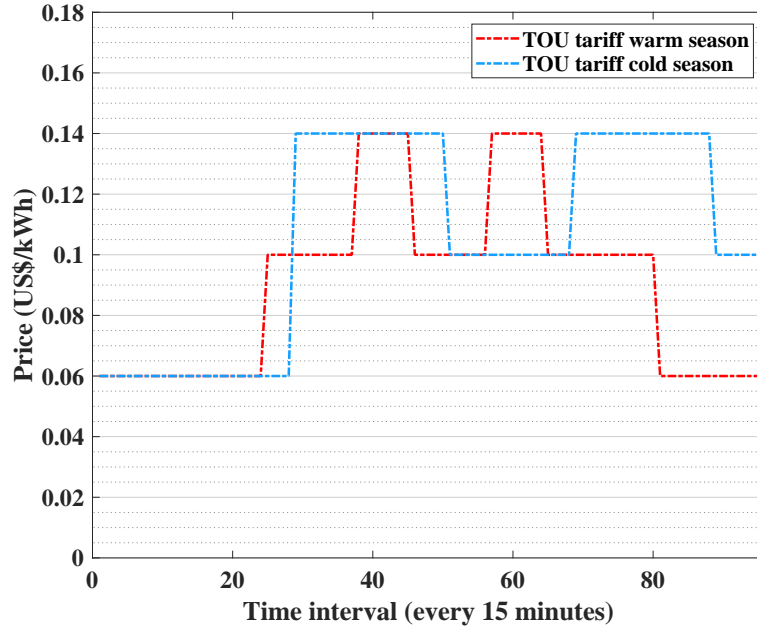
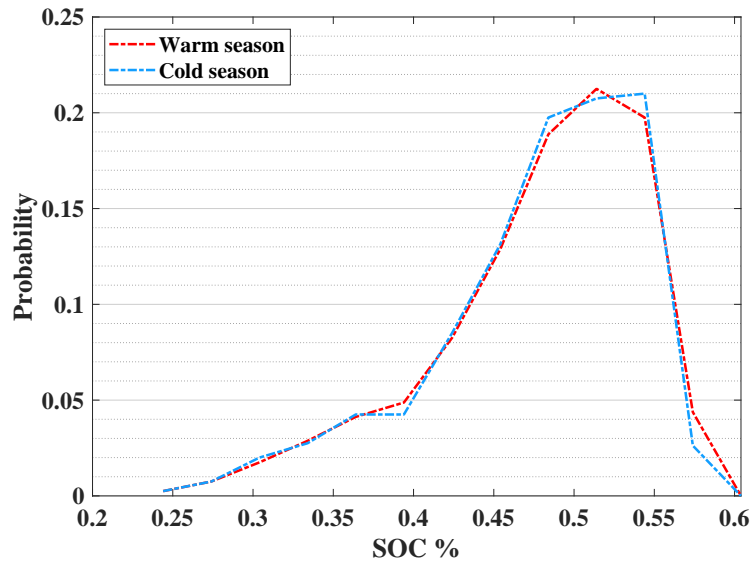


Figure 11: Electricity tariffs

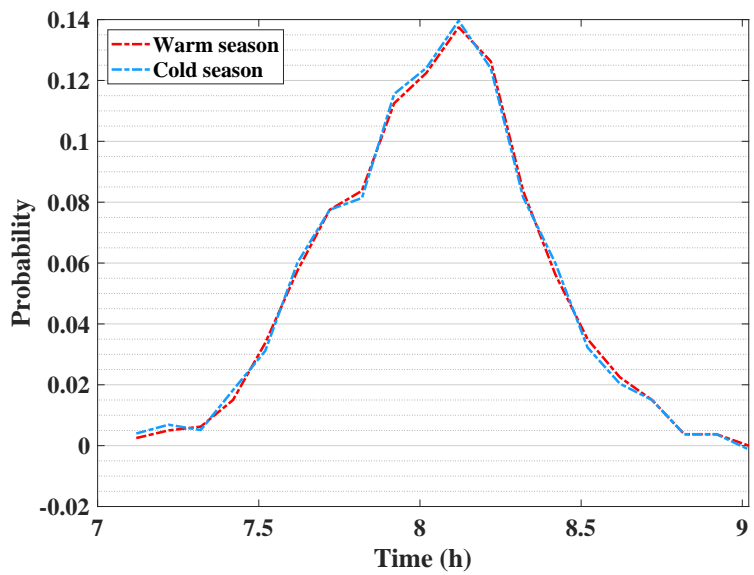
453 As demonstrated in Figure 11, the electricity pricing varies by TOU. In this pa-
 454 per, prices of 0.06 US\$/kWh, 0.1 US\$/kWh and 0.14 US\$/kWh are categorized as
 455 low, moderate and high respectively. In the simulations, it is assumed that EVs are
 456 charged at level 2. Charging of EVs is generally divided into 2 levels [47]. Level 1
 457 charging is commonly used at homes and can charge EVs up to 1.92 KW depending
 458 on the equipment used, whereas level 2 charging is mostly used in PLs and has the
 459 ability to charge EVs up to 19.2 KW depending on the equipment used. In this pa-
 460 per, 5kWh is considered as the maximum charge rate. To increase the accuracy of
 461 the simulations, optimization time intervals of 15 minutes are considered. i.e. the
 462 charge and discharge rate of the active and reactive power varies every 15 minutes.

463 4.2. Results of the route mapping

464 According to the route mapping performed for EVs, the probability distribution
 465 of their SoC and arrival times at the PLs, for cold and warm seasons are shown in
 466 Figure 12.



(a) probability distribution of EVs' SoC



(b) probability distribution of EVs' arrival time

Figure 12: Probability distribution of EVs' SoC and arrival times

467 4.3. Scenario description

468 In this section, 5 different scenarios (SC) are considered for the day-ahead op-
469 timal charging program.

- 470 ✓ Scenario 1 (**SC1**): no EVs participate in the day-ahead optimal charging pro-
471 gram. (base scenario)
- 472 ✓ Scenario 2 (**SC2**): EVs are charged at a constant rate of 1 KW as soon as they
473 enter the PLs (uncontrolled charging).
- 474 ✓ Scenario 3 (**SC3**): the active power exchange between EVs and the grid is
475 optimized and only the benefit of EV owners is taken into account (the cost
476 function is OF_1).
- 477 ✓ Scenario 4 (**SC4**): the active power exchange between EVs and the grid is
478 optimized and only the benefit of SO is taken into account (the cost function
479 is OF_2).
- 480 ✓ Scenario 5 (**SC5**): the active and reactive power exchange between EVs and
481 the grid is optimized taking into account the simultaneous benefit of EV own-
482 ers and SO.

483 4.3.1. Daily profile of the network's active and reactive power, losses and power factor

484 Figure 13 shows the daily active power profile of the network under study. In
485 **SC1**, the daily load of the network is shown without the presence of EVs. In **SC2**,
486 it is demonstrated that EVs are charged as soon as they enter the PLs, creating a
487 morning peak which causes problems with meeting network demand. The network
488 demand peak in this scenario is increased by about 8.97% in the warm season and
489 by about 13.42% in the cold season, compared to the base scenario (i.e. **SC1**).
490 Furthermore, the energy exchange between the EVs and the grid is limited to the
491 early hours of EVs being present at the PLs, which leads to the incapability of using
492 the full capacity of this flexible load in the charging program. In **SC3**, in the warm
493 season, considering the benefit of the EV owners, charging is done during the hours
494 when the average price of electricity is moderate, which creates a larger peak in
495 the electricity network. In the cold season however, when EVs reach the parking
496 lots, the electricity price is high, as a result, EVs wait until the price of electricity

497 goes down and then start charging. In this scenario, the network demand peak
498 has increased by about 24.5% in the warm season. This significant increase in
499 the network demand peak in the warm season, causes problems such as difficulty
500 meeting network demand by the SO and damage to power equipment. Due to the
501 negative impact of V2G power exchange on the battery of EVs and consequently
502 a decrease in the battery lifespan and considering the price profile, V2G power
503 exchange does not occur at the network demand peak in this scenario. In **SC4**,
504 charging of EVs is done in line with the benefit of the SO and thus, In the warm
505 season, EVs are charged during the hours when the electricity price is moderate
506 and are discharged during peak hours of the load and electricity price. Therefore,
507 network losses and costs are reduced during these hours, and then to compensate
508 for the discharge power and reach the desired SoC when leaving the PLs, EVs are
509 charged again during the hours of low network demand. This will create a peak
510 in the network in the upcoming hours. This increase in the network demand peak
511 is about 4.73%, in the warm season, compared to the base scenario. In the cold
512 season, when the EVs reach the parking lots, due to the high electricity price, they
513 discharge subject to certain constraints. This injection of active power from EVs
514 into the grid is done in an effort to reduce network losses. Then, when the price of
515 electricity goes down, EVs start charging, subject to charging constraints. In **SC5**,
516 charging of EVs is done taking into account the simultaneous benefit of EV owners
517 and the SO. Therefore, in both cold and warm seasons, EVs are charged during hours
518 of moderate electricity price and also the exchange of active and reactive power
519 continues until the last hours of EVs' presence at the PLs. As a result, the new peak
520 created in the network is very small compared to the base scenario (about 0.81%
521 in the warm season), which has a positive effect on reducing losses and meeting
522 network demand. Furthermore, the charging of EVs is more uniform, which in turn
523 can improve the lifespan of network transformers.

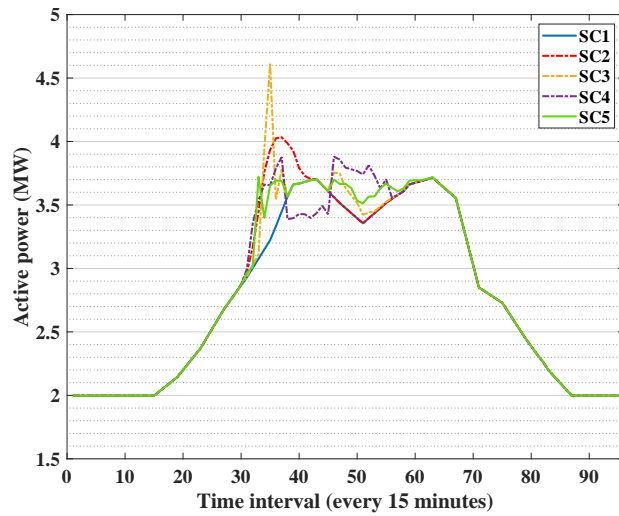
524 In the cold season, charging of EVs occurs during the hours of lowest demand,
525 therefore, the demand peak remains unchanged in **SC3- SC5** compared to the base
526 scenario. Moreover, the lowest network demand peak in the warm season (about
527 0.27%, compared to the base scenario) belongs to **SC5**. **SC2** and **SC5** indicate the

528 worst and best scenarios, respectively in terms of demand response. Moreover, the
529 average daily active power of the network is the same in **SC2- SC5** (since the net-
530 work load is constant and 800 EVs must be charged subject to charging constraints)
531 and has increased by about 1.42% and 1.46%, in the warm and cold seasons respec-
532 tively, compared to the base scenario.

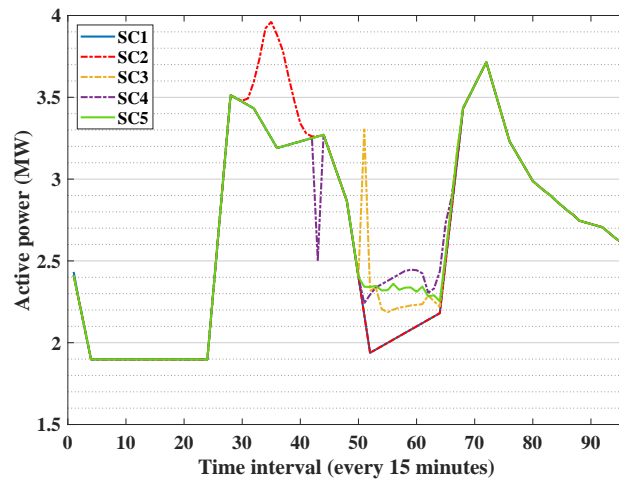
533 Figure 14 demonstrates the daily reactive power profile. As mentioned before,
534 the exchange of reactive power between EVs does not occur in **SC2- SC4** and there-
535 fore the reactive power profile in these scenarios is the same as that of **SC1** (i.e. the
536 base scenario). However, in **SC5** reactive power is injected to the grid by EVs, in
537 both warm and cold seasons. Therefore the average daily reactive power has de-
538 creased by about 19.94% and 23.11%, in the warm and cold seasons, respectively,
539 compared to the base scenario. This decrease in the reactive power exchange not
540 only reduces the costs of reactive losses but also improves network voltage.

541 Figure 15 shows the profile of daily network losses. These losses include the
542 sum of active and reactive power losses of the network. As can be seen, in **SC1-**
543 **SC4** this profile is similar to the active power profile (Figure 13), since in these
544 scenarios no exchange of reactive power with the grid occurs and the loss profile
545 is only a function of the active power profile. Therefore it is observed that the
546 average daily losses, in warm and cold seasons, have increased by about 2.94%
547 and 3.15%, respectively, in **SC2- SC4** compared to the base scenario. (The average
548 daily losses are the same in **SC2- SC4**, however the average cost of losses varies in
549 each scenario depending on the price profile, which is discussed later in Table 3).
550 In **SC5** however, the situation is different and due to the injection of reactive power
551 from the EVs to the grid, the average daily network losses have decreased by about
552 8.04% and 8.32%, in warm and cold seasons, respectively, compared to the base
553 scenario.

554 Finally, the network's daily power factor (PF) profile is demonstrated in Fig-
555 ure 16. PF describes the ratio of network's active power to its apparent power. As
556 this value approaches 1, the network's performance becomes more efficient. As can
557 be seen in Figure 16, in **SC5** the PF is close to 1 during the hours of EVs' presence
558 at the PLs which is due to the decrease in the reactive power during those hours.

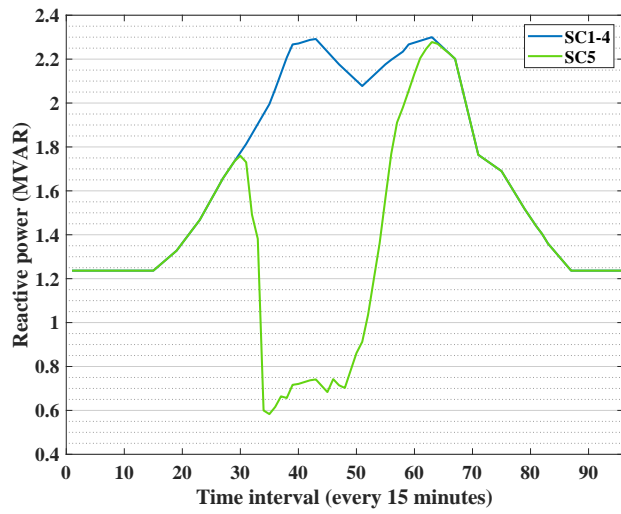


(a) Warm season

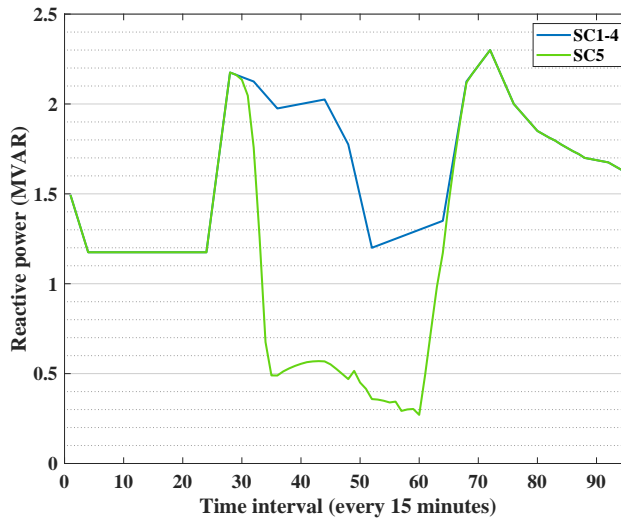


(b) Cold season

Figure 13: Daily active power profile

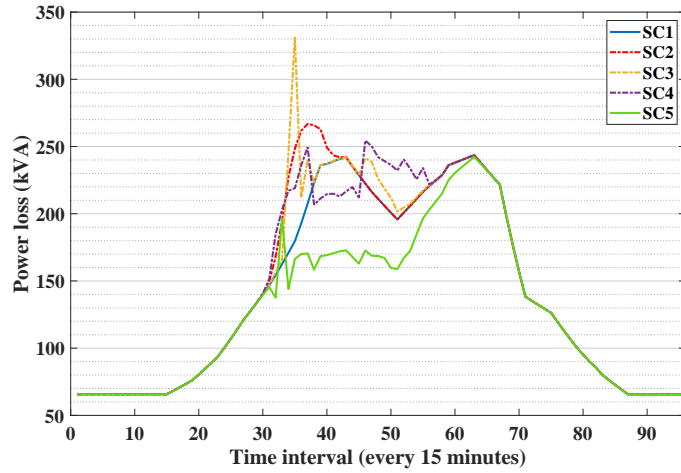


(a) Warm season

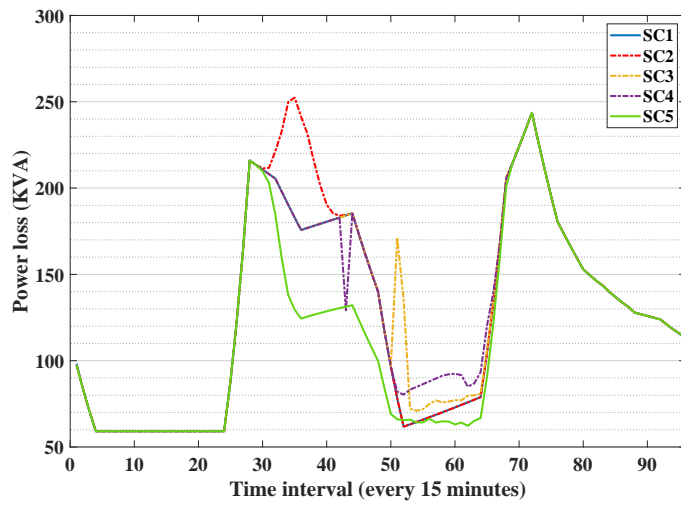


(b) Cold season

Figure 14: Daily reactive power profile

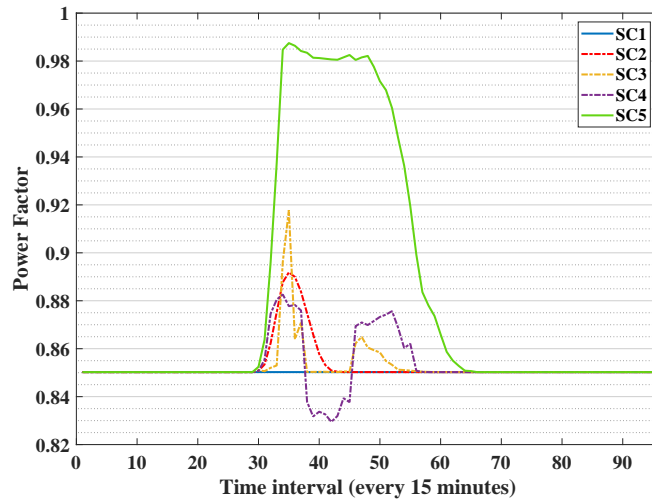


(a) Warm season

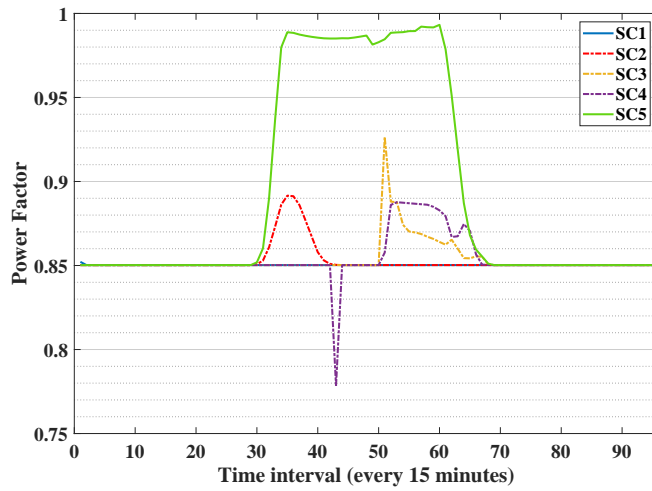


(b) Cold season

Figure 15: Daily network losses profile



(a) Warm season



(b) Cold season

Figure 16: Daily power factor profile

559 4.3.2. Examining the benefits of EV owners in different scenarios

560 In this section, the benefits of the EV owners can be studied in terms of the two
 561 following categories:

- 562 1. Charging costs
- 563 2. Battery wear costs

564 The importance of battery wear costs is that EV owners would have to replace
565 their batteries whenever their EV battery life expires. Therefore, the EV owners
566 would reap more benefits if these batteries lasted longer. It should be noted that
567 all costs discussed for examining the benefits of the EVs and SO, are specific to the
568 time of EVs' presence in the framework.

569 Costs of EV battery wear: In **SC2**, **SC3** and **SC5**, considering the fact that EVs
570 do not inject active power into the grid, the cost of battery wear is only related to
571 charging EVs and is almost the same in these three scenarios. However, in **SC4**, due
572 to the injection of active power into the grid, the cost of battery wear is increased
573 by 26.66% and 10.12% in warm and cold seasons, respectively, compared to the
574 other three scenarios.

575 Costs of charging EVs: in **SC2**, given that EV charging is partly done at the
576 peak of electricity price, the charging costs are the highest in this scenario and are
577 increased in the warm season by 15.6%, 39.3% and 15.46%, and in the cold sea-
578 son by 50.84%, 56.97% and 50.58% compared to **SC3**, **SC4** and **SC5**, respectively.
579 Meanwhile, in **SC4**, EVs inject active power into the grid; in fact in this scenario,
580 EVs sell power to the grid at the peak of electricity price and are recharged later
581 when the prices drop. Therefore their charging costs are improved over **SC2**, **SC3**
582 and **SC5** respectively by 28.21%, 17.02% and 17.12% in the warm season and by
583 36.29%, 3.91% and 4.07% in the cold season.

584 Regarding the total costs of EV owners, it can be noted that in **SC3**, the op-
585 timization is done based solely on the benefits of the EV owners. Therefore the
586 lowest costs for EV owners result from this scenario which compared to **SC2**, **SC4**
587 and **SC5** show an improvement of 4%, 13.15% and 0.03%, respectively in the warm
588 season and the results obtained from the load profile of the cold season indicate an
589 improvement of 11.82%, 6.03% and 0.05% respectively. It can be observed that
590 despite the lower charging costs, the highest costs for EV owners, results from **SC4**,
591 which indicates that with the defined electricity tariff and the price of lithium bat-
592 teries, participating in the V2G market is not in the interest of EV owners. The costs
593 related to charging EVs and their battery wear in **SC2**- **SC5** are demonstrated in
594 Table 2 for the load profiles of cold and warm seasons.

Table 2: Costs related to charging EVs and their battery wear in SC2-5 in cold and warm seasons

		<u>SC2</u>	<u>SC3</u>	<u>SC4</u>	<u>SC5</u>
Warm Season	Battery cost (\$)	1043.4	1043.4	1321.54	1043.4
	Electricity cost (\$)	439.4	380.11	315.43	380.58
	Total cost (\$)	1482.8	1423.51	1638.97	1423.98
Cold Season	Battery cost (\$)	1036.4	1036.4	1141.3	1036.4
	Electricity cost (\$)	559.99	371.25	356.75	371.89
	Total cost (\$)	1596.39	1407.65	1498.05	1408.29

595 *4.3.3. Examining the benefits of the SO in different scenarios*

596 Regarding the operating costs of transformers, it can be stated that in SC5, the
597 load profile is more smooth and the network demand peak is lower compared to
598 the other scenarios. Therefore, in this scenario, for the warm season, the operating
599 costs of transformers are decreased by 0.9%, 0.86% and 1.74%, compared to SC2,
600 SC3 and SC4, respectively. In the cold season, this value is decreased by 2.97%,
601 2.1% and 32%, respectively.

602 The cost of losses in SC4, through optimizing the active power exchange is re-
603 duced by 2.35% in the warm season and by 4.62% in the cold season compared to
604 the uncontrolled case (SC2). This is because the optimization in SC4 is done in line
605 with the benefits of the SO. Meanwhile, in SC5, with simultaneous optimization of
606 the active and reactive power exchange between EVs and the grid, the cost of losses
607 is reduced by 16.72%, 16.36% and 14.72% in the warm season and by 24.93%,
608 21.87% and 21.29% in the cold season respectively, compared to SC2, SC3 and
609 SC4.

610 Regarding the total costs of the SO, it can be observed that SC5 yields the lowest
611 costs, which compared to SC2, SC3 and SC4 is decreased by 15.42%, 15.08% and
612 13.6% respectively in the warm season. In the cold season this value is decreased
613 by 22.28%, 19.42% and 18.71% respectively. The operating costs of transformers
614 and loss costs for the SO in SC2- SC5 are demonstrated in Table 3 for cold and
615 warm seasons.

Table 3: Operating costs of transformers and cost of daily losses for SO in **SC2-5** in cold and warm seasons

		SC2	SC3	SC4	SC5
Warm Season	Loss cost (\$)	259.54	258.42	253.44	216.14
	Transformer cost (\$)	23.34	23.33	23.54	23.13
	Total cost (\$)	282.88	281.75	276.98	239.27
Cold Season	Loss cost (\$)	188.87	181.47	180.14	141.79
	Transformer cost (\$)	25.91	25.68	25.22	25.14
	Total cost (\$)	214.78	207.15	205.36	166.93

616 4.3.4. Sensitivity analysis of the performed optimization to the number of participat-
617 ing EVs

618 In this section, sensitivity analysis to the number of EVs for the load profile of
619 the cold season is discussed. In 4 different cases, different numbers of EVs are
620 considered and **SC2** and **SC5** are compared in terms of battery, electricity, loss and
621 transformer costs. The results are demonstrated in Table 4 and all costs are specific
622 to the time of EVs' presence in the framework. Based on the results of this table,
623 the costs in **SC2** (uncontrolled scenario) are higher than those of **SC5**. In both
624 scenarios, due to the lack of active power injection from the EVs into the grid,
625 battery degradation cost only exists when the batteries are charging and therefore,
626 this cost is the same in both scenarios for all cases. In Cases 1, 2, 3 and 4 the
627 cost of electricity in **SC5** is decreased by 33.37%, 34.09%, 33.59% and 33.88%,
628 respectively, compared to **SC2**. This is because in **SC2**, Evs are charged when the
629 price of electricity is high. In **SC5**, the loss cost for the network in cases 1, 2, 3 and 4,
630 is decreased by 7.28%, 16.13%, 24.93% and 28.48% compared to **SC2**, due to the
631 reactive power injection from EVs into the grid. Transformer costs are also higher
632 in **SC2**, since in **SC5**, EVs are charged evenly and without peaks, as peaks reduce
633 the lifespan of network transformers. The decrease in the transformer cost in **SC5**
634 is 1.66%, 2.42%, 2.97% and 2.73% for the four cases, respectively. Moreover, the
635 total costs in sc5 are reduced by 10.12%, 12.47%, 13.03% and 13.11% in cases 1,

636 2, 3 and 4, respectively.

Table 4: Sensitivity analysis for the load profile of cold season

Number of EVs	Scenarios	Battery Cost (\$)	Electricity Cost (\$)	Loss Cost (\$)	Transformer Cost (\$)	Total Costs (\$)
Case1: 200 EV	<u>SC2</u>	262.29	140.87	178.81	25.35	607.32
	<u>SC5</u>	262.29	93.86	165.8	24.93	545.88
Case2: 400 EV	<u>SC2</u>	515.86	278.84	182.02	25.63	1002.35
	<u>SC5</u>	515.86	183.79	152.66	25.01	877.32
Case3: 800 EV	<u>SC2</u>	1036.4	559.99	188.87	25.91	1851.17
	<u>SC5</u>	1036.4	371.89	141.79	25.14	1575.22
Case4: 1000 EV	<u>SC2</u>	1302.6	691.66	192.36	26.04	2213.02
	<u>SC5</u>	1302.6	461.18	142.10	25.33	1931.21

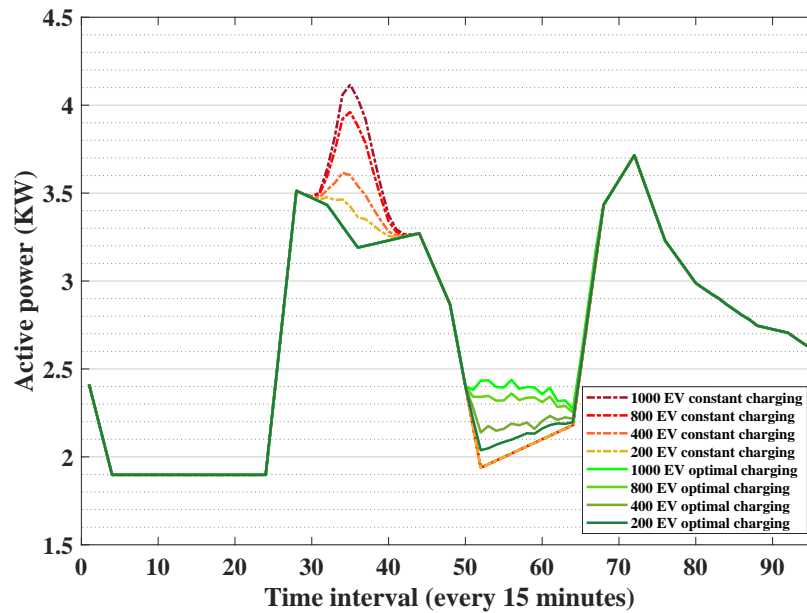


Figure 17: Sensitivity analysis for the load profile of cold season

637 **5. Conclusion**

638 In this paper, a framework for day-ahead optimal charging of EVs has been pre-
 639 sented. Firstly, considering four effective factors on electrical energy consumption

640 of EVs, including vehicle speed, ambient temperature, wind speed and road grade,
641 a route mapping algorithm has been implemented so as to provide better services
642 to EV owners. Next, based on the performed route mapping and time of arrival at
643 the selected PLs for each EV, a method has been proposed for the optimal charg-
644 ing of EVs, through optimizing active and reactive power exchange between EVs
645 and the grid, using a hybrid interior-point optimization approach. Moreover, this
646 method considered the simultaneous benefit of EV owners, PLOs and SO. The simu-
647 lations have been carried out utilizing traffic information from the city of Kowloon
648 and a standard IEEE 33 bus system. Different scenarios have been investigated for
649 load profiles of cold and warm seasons, which show that the proposed scenario
650 yields a better performance than the uncontrolled scenario. In the optimal charg-
651 ing method, the cost of charging EVs and network losses during the hours of EVs'
652 presence in the framework, were reduced up to 33.6% and 24.93% respectively
653 compared to the uncontrolled scenario. Furthermore, the lifespan of the power
654 transformers has improved up to 2.97% compared to the uncontrolled scenario.
655 The main results obtained from this paper can be summarized as follows:

- 656 1. Providing a new framework for day-ahead optimal charging of EVs
- 657 2. Presenting a new route mapping algorithm with the utilization of cloud sys-
658 tems to provide EVs with better services
- 659 3. Introducing an optimal method of charging EVs, considering the benefits of
660 the EV owners and SO simultaneously.

661 The proposed framework was able to significantly reduce the costs of losses and
662 charging EVs, which could play an important role in reducing the costs of the SO
663 and EV owners in the future.

References

- [1] Z. Wang, P. Jochem, W. Fichtner, A scenario-based stochastic optimization model for charging scheduling of electric vehicles under uncertainties of vehicle availability and charging demand, *Journal of Cleaner Production* 254 (2020) 119886.

- [2] M. Ahrabi, M. Abedi, H. Nafisi, M. A. Mirzaei, B. Mohammadi-Ivatloo, M. Marzband, Evaluating the effect of electric vehicle parking lots in transmission-constrained ac unit commitment under a hybrid igdt-stochastic approach, *International Journal of Electrical Power Energy Systems* 125 (2021) 106546.
- [3] H. Jahangir, H. Tayarani, A. Ahmadian, M. A. Golkar, J. Miret, M. Tayarani, H. O. Gao, Charging demand of plug-in electric vehicles: Forecasting travel behavior based on a novel rough artificial neural network approach, *Journal of Cleaner Production* 229 (2019) 1029–1044.
- [4] M. Li, H. He, L. Feng, Y. Chen, M. Yan, Hierarchical predictive energy management of hybrid electric buses based on driver information, *Journal of Cleaner Production* 269 (2020) 122374.
- [5] H. Guo, X. Wang, L. Li, State-of-charge-constraint-based energy management strategy of plug-in hybrid electric vehicle with bus route, *Energy Conversion and Management* 199 (2019) 111972.
- [6] P. Aliasghari, B. Mohammadi-Ivatloo, M. Alipour, M. Abapour, K. Zare, Optimal scheduling of plug-in electric vehicles and renewable micro-grid in energy and reserve markets considering demand response program, *Journal of Cleaner Production* 186 (2018) 293–303.
- [7] P. Khayyer, J. Wollaeger, S. Onori, V. Marano, Özgüner, G. Rizzoni, Analysis of impact factors for plug-in hybrid electric vehicles energy management, in: 2012 15th International IEEE Conference on Intelligent Transportation Systems, 2012, pp. 1061–1066.
- [8] W. Chiu, J. Hsieh, C. Chen, Pareto optimal demand response based on energy costs and load factor in smart grid, *IEEE Transactions on Industrial Informatics* 16 (3) (2020) 1811–1822.
- [9] H. Nafisi, Investigation on distribution transformer loss-of-life due to plug-in

hybrid electric vehicles charging, *International Journal of Ambient Energy* 0 (2019) 1–19.

- [10] N. T. Milas, E. C. Tatakis, Charging station selection through the analytic hierarchy process enabled by opc-ua for vehicle-to-grid communications, in: 2019 21st European Conference on Power Electronics and Applications (EPE '19 ECCE Europe), 2019, pp. P1–P10.
- [11] R. Das, Y. Wang, G. Putrus, R. Kotter, M. Marzband, B. Herteleer, J. Warmerdam, Multi-objective techno-economic-environmental optimisation of electric vehicle for energy services, *Applied Energy* 257 (2020) 113965.
- [12] M. Tavakoli, F. Shokridehaki, M. Marzband, R. Godina, E. Pouresmaeil, A two stage hierarchical control approach for the optimal energy management in commercial building microgrids based on local wind power and pevs, *Sustainable Cities and Society* 41 (2018) 332 – 340.
- [13] J. Chen, X. Huang, S. Tian, Y. Cao, B. Huang, X. Luo, W. Yu, Electric vehicle charging schedule considering user's charging selection from economics, *IET Generation, Transmission Distribution* 13 (15) (2019) 3388–3396.
- [14] N. Bañol Arias, S. Hashemi, P B. Andersen, C. Træholt, R. Romero, Assessment of economic benefits for ev owners participating in the primary frequency regulation markets, *International Journal of Electrical Power & Energy Systems* 120 (2020) 105985.
- [15] Y. Luo, T. Zhu, S. Wan, S. Zhang, K. Li, Optimal charging scheduling for large-scale ev (electric vehicle) deployment based on the interaction of the smart-grid and intelligent-transport systems, *Energy* 97 (2016) 359–368.
- [16] B. Khaki, C. Chu, R. Gadh, Hierarchical distributed framework for EV charging scheduling using exchange problem, *Applied Energy* 241 (2019) 461–471.
- [17] M. Mozaffari, H. Askarian Abyaneh, M. Jooshaki, M. Moeini-Aghtaie, Joint expansion planning studies of ev parking lots placement and distribution network, *IEEE Transactions on Industrial Informatics* 16 (10) (2020) 6455–6465.

- [18] M. H. Amini, M. P. Moghaddam, O. Karabasoglu, Simultaneous allocation of electric vehicles' parking lots and distributed renewable resources in smart power distribution networks, *Sustainable Cities and Society* 28 (2017) 332–342.
- [19] M. A. Kazemi, M. Sedighizadeh, M. J. Mirzaei, O. Homaei, Optimal siting and sizing of distribution system operator owned ev parking lots, *Applied Energy* 179 (2016) 1176–1184.
- [20] D. S. Markovic, D. Zivkovic, I. Branovic, R. Popovic, D. Cvetkovic, Smart power grid and cloud computing, *Renewable and Sustainable Energy Reviews* 24 (2013) 566–577.
- [21] M. Mierau, S. Fey, R. Kohrs, C. Wittwer, Communication solutions for a cloud-based charging management system for a fleet of shared-use electric vehicles, in: *2013 World Electric Vehicle Symposium and Exhibition (EVS27)*, 2013, pp. 1–11.
- [22] V. Chang, M. Ramachandran, Towards achieving data security with the cloud computing adoption framework, *IEEE Transactions on Services Computing* 9 (1) (2016) 138–151.
- [23] M. M. Hussain, M. S. Alam, M. S. Beg, Plug-in electric vehicle to cloud data analytics for charging management, *International Journal of Engineering & Technology* 9 (2017) 361–370.
- [24] M. Baum, J. Dibbelt, A. Gemsa, D. Wagner, Towards route planning algorithms for electric vehicles with realistic constraints, *Computer Science - Research and Development* 31 (2017) 361–370.
- [25] Z. He, L. Zhao, The comparison of four uav path planning algorithms based on geometry search algorithm, in: *2017 9th International Conference on Intelligent Human-Machine Systems and Cybernetics (IHMSC)*, Vol. 2, 2017, pp. 33–36.

- [26] P. E. Hart, N. J. Nilsson, B. Raphael, A formal basis for the heuristic determination of minimum cost paths, *IEEE Transactions on Systems Science and Cybernetics* 4 (2) (1968) 100–107.
- [27] W. Zeng, R. Church, Finding shortest paths on real road networks: The case for a, *International Journal of Geographical Information Science* 23 (2009) 531–543.
- [28] Yin Chao, Wang Hongxia, Developed dijkstra shortest path search algorithm and simulation, in: 2010 International Conference On Computer Design and Applications, Vol. 1, 2010, pp. V1–116–V1–119.
- [29] H. I. Kang, B. Lee, K. Kim, Path planning algorithm using the particle swarm optimization and the improved dijkstra algorithm, in: 2008 IEEE Pacific-Asia Workshop on Computational Intelligence and Industrial Application, Vol. 2, 2008, pp. 1002–1004.
- [30] Z. Fuhao, L. Jiping, An algorithm of shortest path based on dijkstra for huge data, in: 2009 Sixth International Conference on Fuzzy Systems and Knowledge Discovery, Vol. 4, 2009, pp. 244–247.
- [31] T. Yuksel, J. J. Michalek, Effects of regional temperature on electric vehicle efficiency, range, and emissions in the united states, *Environmental Science & Technology* 49 (6) (2015) 3974–3980.
- [32] S. M. Agah, H. A. Abyaneh, Distribution transformer loss-of-life reduction by increasing penetration of distributed generation, *IEEE Transactions on Power Delivery* 26 (2) (2011) 1128–1136.
- [33] H. Farzin, M. Fotuhi-Firuzabad, M. Moeini-Aghaie, A practical scheme to involve degradation cost of lithium-ion batteries in vehicle-to-grid applications, *IEEE Transactions on Sustainable Energy* 7 (4) (2016) 1730–1738.
- [34] S. Han, S. Han, H. Aki, A practical battery wear model for electric vehicle charging applications, *Applied Energy* 113 (2014) 1100 – 1108.

- [35] S. B. Peterson, J. Apt, J. Whitacre, Lithium-ion battery cell degradation resulting from realistic vehicle and vehicle-to-grid utilization, *Journal of Power Sources* 195 (8) (2010) 2385–2392.
- [36] S. S. K. Madahi, H. Nafisi, H. A. Abyaneh, M. Marzband, Co-optimization of energy losses and transformer operating costs based on smart charging algorithm for plug-in electric vehicle parking lots, *IEEE Transactions on Transportation Electrification*, Advance online publication, (2020). doi:10.1109/TTE.2020.3020690.
- [37] M. Gertz, J. Nocedal, A. Sartendar, A starting point strategy for nonlinear interior methods, *Applied Mathematics Letters* 17 (8) (2004) 945–952.
- [38] L. Jourdan, M. Basseur, E.-G. Talbi, Hybridizing exact methods and metaheuristics: A taxonomy, *European Journal of Operational Research* 199 (3) (2009) 620–629.
- [39] B. Mansoornejad, N. Mostoufi, F. Jalali-Farahani, A hybrid ga–sqp optimization technique for determination of kinetic parameters of hydrogenation reactions, *Computers Chemical Engineering* 32 (7) (2008) 1447–1455.
- [40] <https://data.gov.hk>, https://data.gov.hk/en-data/dataset/hk-td-sm_1-traffic-speed-map, accessed: 2018-07-01.
- [41] Kowloon, hong kong 14 day weather forecast., <https://www.timeanddate.com/weather/china/kowloon/ext.>, accessed: 2018-07-01.
- [42] M. R. Sarker, D. J. Olsen, M. A. Ortega-Vazquez, Co-optimization of distribution transformer aging and energy arbitrage using electric vehicles, *IEEE Transactions on Smart Grid* (2017).
- [43] A. Gailani, M. Al-Greer, M. Short, T. Crosbie, Degradation cost analysis of li-ion batteries in the capacity market with different degradation models, *Electronics* 9 (1) (2020).

- [44] K. Liu, X. Hu, Z. Yang, Y. Xie, S. Feng, Lithium-ion battery charging management considering economic costs of electrical energy loss and battery degradation, *Energy Conversion and Management* 195 (2019) 167 – 179.
- [45] Q. Tan, M. Wang, Y. Deng, H. Yang, R. Rao, X. Zhang, The Cultivation of Electric Vehicles Market in China: Dilemma and Solution, *Sustainability* 6 (2014).
- [46] Y.-J. Ma, M.-Y. Zhai, Day-ahead prediction of microgrid electricity demand using a hybrid artificial intelligence model, *Processes* 7 (6) (2019).
- [47] M. Muratori, Impact of uncoordinated plug-in electric vehicle charging on residential power demand, *Nat. Energy* 3 (2018) 193–201.